RSC Advances

PAPER

View Article Online
View Journal | View Issue

Cite this: *RSC Adv.*, 2019, **9**, 39410

Quinoline-triazole hybrids inhibit falcipain-2 and arrest the development of *Plasmodium falciparum* at the trophozoite stage†

Anju Singh,‡[a] Md Kalamuddin,‡[b] Asif Mohmmed,[b] Pawan Malhotra*[b] and Nasimul Hoda *[a]

Received 21st August 2019
Accepted 9th November 2019

DOI: 10.1039/c9ra06571g

rsc.li/rsc-advances

Falcipain-2 (FP2) is a papain family cysteine protease and a key member of the hemoglobin degradation pathway, a process that is required at erythrocytic stages of *Plasmodium falciparum* to obtain amino acids. In this study, we report a set of 10 quinoline-triazole-based compounds (**T1–T10**) which exhibit a good binding affinity for FP2, inhibit its catalytic activity at micromolar concentrations and thereby arrest the parasite growth. Compounds **T4** and **T7** inhibited FP2 with IC_{50} values of 16.16 μM and 25.64 μM respectively. Both the compounds **T4** and **T7** arrested the development of *P. falciparum* at the trophozoite stage with an EC_{50} value 21.89 μM and 49.88 μM. These compounds also showed morphological and food-vacuole abnormalities like **E-64**, a known inhibitor of FP2. Our results thus identify the quinoline-triazole-based compounds as a probable starting point for the design of FP2 inhibitors and they should be further investigated as potential antimalarial agents.

1. Introduction

Malaria is a major life-threatening disease caused by *Plasmodium* parasites. According to the WHO 2018 report, *Plasmodium* parasites affect 216 million people each year. In 2017, 445 000 people, mostly children, died due to malaria. Malaria is caused by different species of *Plasmodium* protozoan, among which *P. falciparum* is responsible for causing the most deaths due to malaria, especially among children under the age of 5 in Africa. The malaria parasite follows a complex life cycle that includes many formative stages in the human host and mosquito vector, which contributes greatly to the challenge of its treatment.[1–4]

Artemisinin in combination with other drugs (artemisinin-combination therapy, ACT) is the first-choice treatment for malaria worldwide. However, recently resistance to most of the antimalarial drugs including ACTs is being reported in different geographical areas.[5] Therefore, identification of novel multi-stage drug targets with new modes of action is required to develop new antimalarials against these resistant parasites.

Plasmodium proteases play crucial roles at all stages of the parasite life cycle and are thus potential antimalarial targets.[6] Falcipains (FPs), majorly FP2 and FP3 are unique food vacuole *Plasmodium* cysteine proteases that rapidly cleave hemoglobin, an essential step in asexual blood stage parasite survival. FP2 is also involved in degradation of erythrocyte-membrane cytoskeletal proteins mainly ankyrin and band 4.1.[7,8]

With due course of time and advancement in this field of research, scientific community has developed diverse range of antimalarial drug molecules targeting inhibition of FP2. Gallinamide A (Fig. 1a) leads to swelling of parasite food vacuole when dosed upon cultured *P. falciparum* and cause parasite death.[9,10] "Gallinamide A" analogues have been found to exhibit effective inhibiting ability for FP2, FP3 and for the development of *P. falciparum in vitro*.[11] Along with this, **E64** (Fig. 1b) an epoxide and an important irreversible inhibitor against general cysteine proteases and displayed a significant outcome on growth, adherence and viability of parasite trophozoites.[12] A representative of benzoxaboroles, AN3661 (Fig. 1c), has been found to markedly reduce the FP2 transcripts in malarial parasites.[13] A new class of peptidomimetic inhibitor of FP2 having 1,4-benzodiazepine scaffold (Fig. 1d) joint with vinyl ester, evidenced to be a highly potent and selective FP2 inhibitor.[14] Derivatives of some heteroaryl nitrile with the 5-substituted-2-cyanopyrimidine (Fig. 1e) displayed a potential FP2 inhibition and therefore substantial antiparasitic effect.[15] Natural product hybrids like lactone–chalcone and isatin–chalcone have also been reported to inhibit FP2 through probing the S2 active site pocket of the enzyme.[16] Stilbene–chalcone hybrids have been reported to cause to cause apoptosis in malaria parasite.[17] 4-phenylchalcone based compounds have been observed to inhibit cathepsins B, H

[a]*Drug Design and Synthesis Lab., Department of Chemistry, Jamia Millia Islamia, Jamia Nagar, New Delhi-110025, India. E-mail: nhoda@jmi.ac.in; Fax: +91-11-26985507; Tel: +91-9910200655*

[b]*International Centre for Genetic Engineering and Biotechnology (ICGEB), Aruna Asaf Ali Marg, New Delhi-110067, India. E-mail: pawanm@icgeb.res.in; Tel: +91-11-267423*

† Electronic supplementary information (ESI) available. See DOI: 10.1039/c9ra06571g

‡ These authors contributed equally to this work.

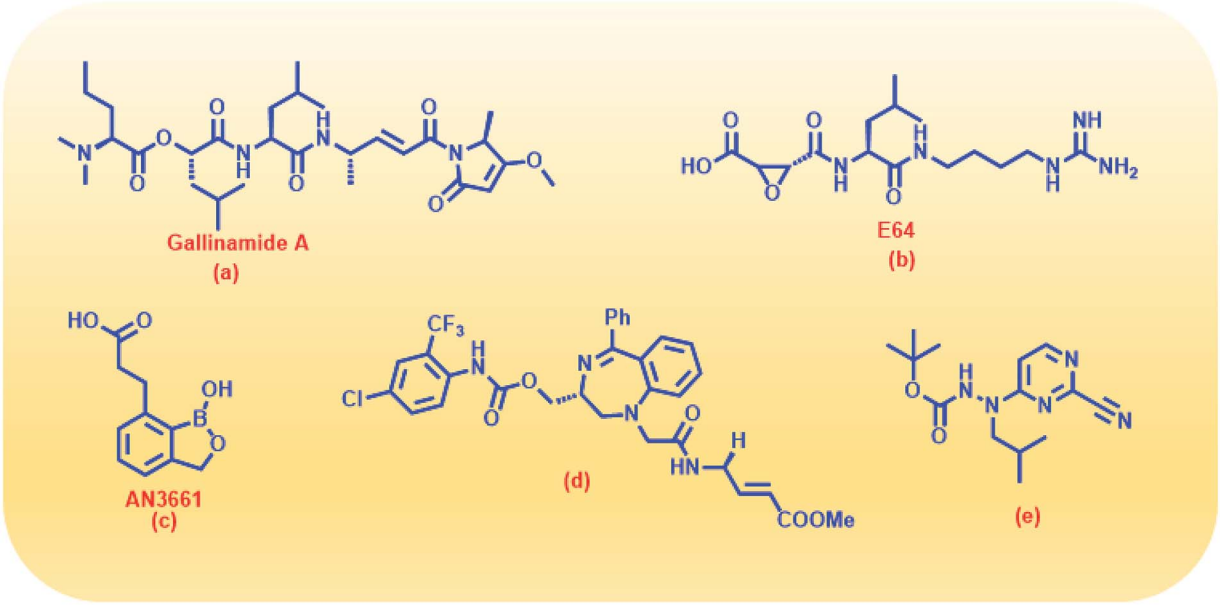

Fig. 1 Structures of some reported FP2 inhibitors.

and L.[18] In addition, coumarin-chalcone have also been reported to be potential bioactive agents.[19] Although plentiful active and efficient FP2 inhibitors in *in vivo* models of malaria have been reported, but none has yet been progressed into human clinical trials.[20–22]

Triazoles are 5-membered heterocyclic class of organic molecules, which exist in two forms, the 1,2,4-triazole and 1,2,5-triazole based on the position of nitrogen atoms. Even though the triazoles have a bright history in pharmacology, it gained more popularity by the copper catalyzed click chemistry. Triazole besides acting as a passive linker also participates as a dominant scaffold to enhance biological activity of drug molecules. Its acceptability as a bioactive scaffold is related to its ability to bind with target receptors by means of H-bonding, π–π stacking and dipole–dipole interactions. In addition, its ability to survive both moderate to acid–base conditions as well as its resistance to metabolic degradation make it an attractive pharmacophore for drug design.[23–25] 1,2,3-Triazole derivatives have been shown to have numerous medicinal values such as antihypertensive, anticancer, antitubercular, anti-inflammatory, antifungal, anticholinergic, antibacterial and antiviral properties.[26–29] These compounds are also known for their anti-MRSA potency[30] over and above powerful antimalarial, anticancer and antidiabetic activities.[31] Fluconazole, voriconazole and itraconazole are some of the important triazole core moiety-based drugs. Recently, admirable triazole-

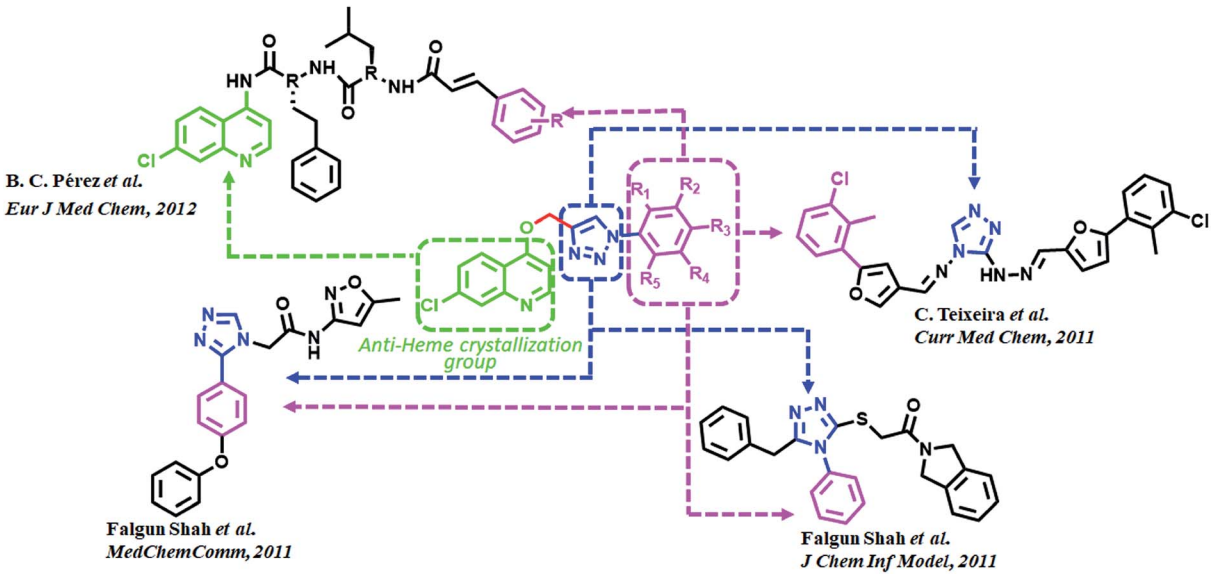

Fig. 2 Rationale for the design and synthesis of triazole-quinoline derivatives as FP2 inhibitors.

Table 1 The computational binding free energies of the designed molecules (**T1–T10**) with (FP2) using ParDOCK[59] and AutoDock Vina program[60]

Compounds	Structures	Computational binding free energy (kcal mol^{-1}) using ParDOCK	Computational binding free energy (kcal mol^{-1}) using AutoDock
T1	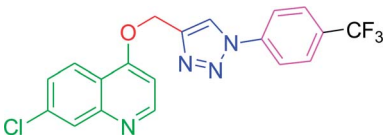	−6.31	−5.7
T2	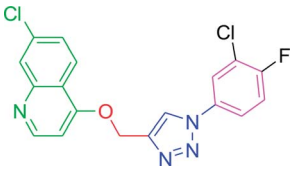	−6.21	−6.8
T3	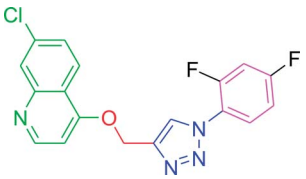	−6.43	−6.6
T4	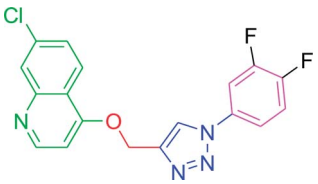	−6.15	−6.9
T5	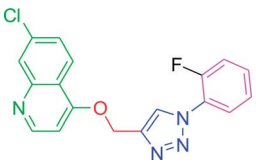	−6.32	−6.4
T6	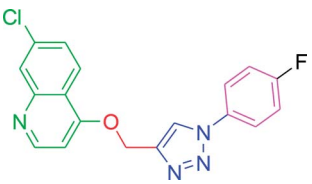	−6.31	−6.7
T7	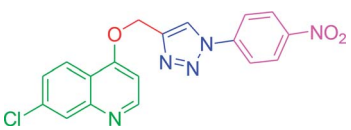	**−7.91**	**−6.7**
T8	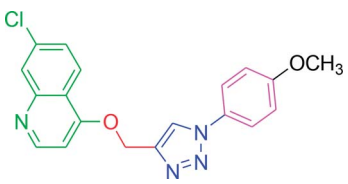	−7.52	−6.5
T9	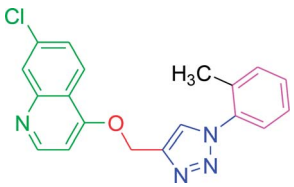	−6.13	−6.1

Table 1 (*Contd.*)

Compounds	Structures	Computational binding free energy (kcal mol^{-1}) using ParDOCK	Computational binding free energy (kcal mol^{-1}) using AutoDock
T10	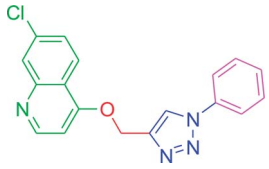	−5.91	−6.5
E64	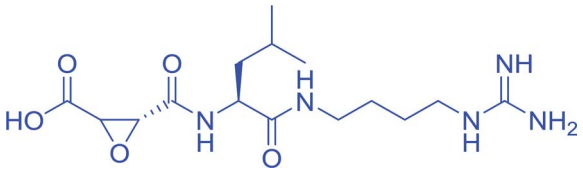	−6.14	−6.9

based FP2 inhibitors have been developed[32–34] among which a few are given in (Fig. 2). Such molecules have been the main source of consideration to design new potential FP2 inhibitors.

Quinoline and its derivatives, have been reported as rich bioactive heterocyclic compounds, which show antimalarial, antibiotic, anticancerous and anti-inflammatory properties.[35–39] Many current antimalarials such as chloroquine, amodiaquine, mefloquine and primaquine have quinoline as core moiety. Ester containing quinoline compounds have also a bright history for antimalarial effect.[40] Quinoline analogues are well known for inhibiting hemozoin formation (heme crystallization).[41–46] These analogues bind with precrystalline forms of heme that can conceivably bring about such inhibition and have been characterized by various spectroscopic methods.[47–49] *N*-(7-chloroquinolinyl-4-aminoalkyl)arylsulfonamides have been found to inhibit hemozoin formation and display promising antimalarial activity.[50] Potential antiplasmodial effect has been reported from short peptide-based compounds with IC_{50} values ranging between 1.4–4.7 mg mL^{-1}.[51] B. C. Pérez and his co-workers reported a set of chloro quinoline containing cinnamic acids as excellent inhibitors of FP2.[52] (Fig. 2).

Based on the previously reported excellent pharmacokinetic characteristics and favorable safety profile of triazole and quinoline derivatives,[53–58] we synthesized a series of chloroquinoline triazole analogues as antimalarial agents. Indeed, we employed the archetypical click reaction: the Huisgen [3 + 2] cycloaddition between alkynes and azides catalyzed by copper(I). Thus, the removal of dynamic proton has helped us to come out with triazoles, which predominately exist in only one isomeric form.

2. Results and discussion

2.1. *In silico* design of potential FP2 inhibitors

The docking results predict the binding affinity ($-\Delta G$ in kcal mol^{-1}) between the ligand and the active site of FP2 (PDB ID 3BPF). Noncovalent interactions like π–π interactions, allyl–π interactions and H-bond interactions were studied. It was found that the alkyl or aryl groups with varying hydrophobicity and electronic environment decided the binding affinity of the ligands to the drug target. The binding free energy ($-\Delta G$) of the designed molecules with FP2 is enlisted in Table 1. The computational binding free energy of complexation of **T7** with the target enzyme was found to be more favorable (−7.91 kcal mol^{-1} as per ParDOCK), indicating its better binding affinity towards the enzyme. From the docking pose of compound **T7** shown in (Fig. 3a), the aromatic π electron cloud of triazole core structure was engaged with Trp43 through π–π stacking interaction. In addition, Cys39 was observed to form strong H-bond with oxygen of nitrobenzene group while as Asn81 formed a H-bond with nitrogen of triazole system. However, the standard FP2 inhibitor: **E64** merely displayed two H-bonds with Asn173 and Gly83 as shown in (Fig. 3b). Since **E64** lacks an aromatic system and is unable to take part in π–π interactions, may be the reason for its less binding affinity with the enzyme than that of **T7**. From various molecular modelling studies, we observed that our designed molecules fix well into the active site grove of FP2 as visualized in (Fig. 3c). However, the standard molecule: **E64** was not observed to fix appropriately into the active site groove of the enzyme (Fig. 3d).

These *in silico* results were also validated with *in vitro* FP2 inhibition and showed a notable agreement; hence such molecules could be used as lead to develop effectual FP2 inhibitors.

2.2. Chemical synthesis

The development of target molecules was accomplished *via* synthetic route shown in Schemes 1–3. In Scheme 1, differently substituted azides (**3**) were synthesized from differently substituted anilines (**1**). In the Scheme 2, 4,7-dichloroquinoline was made to react with propargyl alcohol in presence of sodium hydride and dry dimethylformamide at room temperature to obtain 7-chloro-4-(prop-2-ynyloxy)quinoline (**6**) according to the literature method. In Scheme 3, compounds **3(a-j)** were coupled

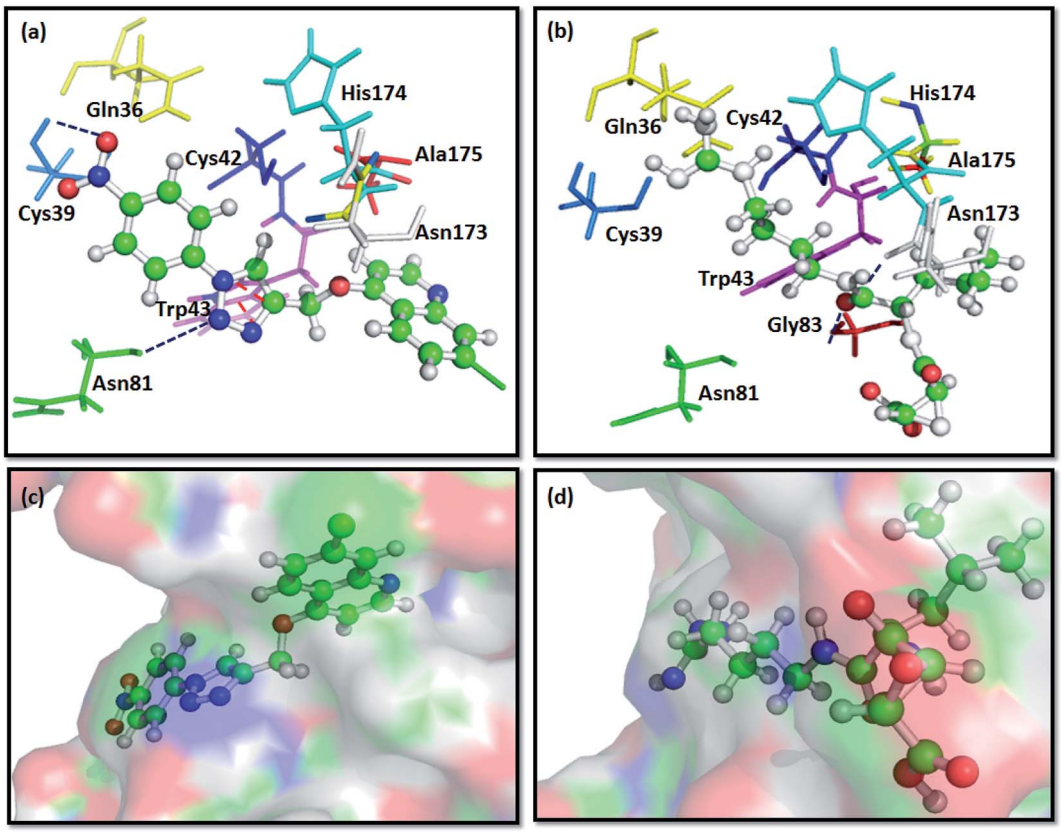

Fig. 3 Docking interactions of **T7** and **E64**, a known standard FP2 inhibitor with FP2:PDB ID 3BPF; (a) binding interaction of compound **T7** with FP2 showing π–π stacking between Trp43 and aromatic triazole ring (represented with red coloured dashes) and two H-bonds between the ligand and Cys39 and Asn81 of FP2 (represented with dark blue coloured dashes). (b) Showing H-bond interaction of **E64** with the Gly83 and Asn173 of FP2 (represented with dark blue coloured dashes). (c) Surface view of **T7** into the active site groove of the enzyme: (d) Surface pose of **E64** with FP2.

with 7-chloro-4-(prop-2-ynyloxy)quinoline complex (**6**) in presence of $CuSO_4 \cdot 5H_2O$, sodium ascorbate, (THF : H_2O, 1 : 2), under the reflux conditions 80 °C for 8 h to obtain our target compounds **7(a-j)**.[61] The structures of these compounds were confirmed through various analytical and spectroscopic methods: (^1H, ^{13}C NMR and mass spectra).

Compound	R_1	R_2	R_3	R_4	R_5
T1	H	CF_3	H	H	H
T2	H	Cl	F	H	H
T3	F	H	F	H	H
T4	H	F	F	H	H
T5	F	H	H	H	H
T6	H	H	F	H	H
T7	H	H	NO_2	H	H
T8	H	H	OCH_3	H	H
T9	CH_3	H	H	H	H
T10	H	H	H	H	H

2.3. Anti-malarial screening of the synthesized compounds

2.3.1. Effect of quinoline-triazole based target compounds on FP2 activity and parasite growth. Based on the docking studies, we next analyzed the effect of triazole-based target compounds on the activity of recombinant FP2 protein as well as on *P. falciparum* growth and development. To investigate the effect of these compounds on FP2 activity, recombinant FP2 was produced by following a protocol described by Shenai, *et al.*[62] and Kumar *et al.*[63] (Fig. 4a) show the expression, purification and refolding of FP2 protein. The refolded protein was catalytically active as it cleaved the enzyloxycarbonyl-Phe-Arg-7-amino-4-methylcoumarin hydrochloride (ZFR-AMC), a substrate of FP2, in a dose dependent manner (Fig. 4b). A set of quinoline-triazole-based compounds (**T1–T10**) were evaluated in the FP2 inhibitory activities, as shown in Table 2, most of the synthesized compounds exhibited IC_{50} values in micromolar range towards the inhibition of FP2. The varying IC_{50} values of the differently substituted triazole compounds may be due to the different electronic properties associated with the substituents. Compound **T7** containing nitro group on the para position of benzene ring, was found to be the best inhibitors of FP2 (IC_{50} = 16.16 μM) in the series. Better inhibitory activity of **T7** may be due to the more electron withdrawing nature of the nitro group. Compounds **T9** and **T8** containing 2-methyl and 4-methoxy at the benzene ring attached to the core triazole showed inhibitory activity: (IC_{50} 20.9 μM and 25.37 μM), respectively. Compounds **T3** and **T4** exhibited almost equal IC_{50} values ~25–26 μM as the benzene ring in both these compounds possess difluoro

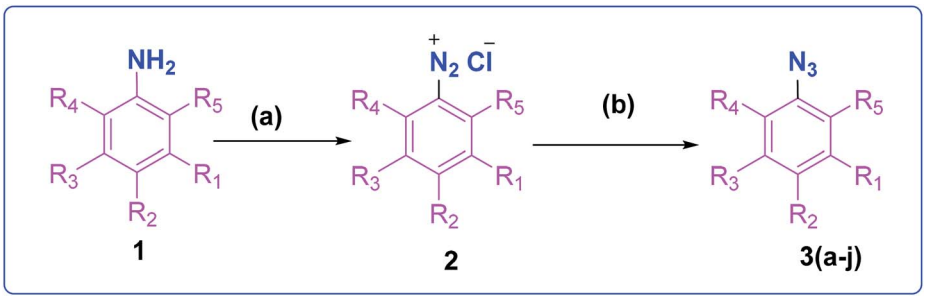

Scheme 1 Synthesis of different aromatic azides. Reagents and conditions: (a) $NaNO_2$, HCl (3 N), ice bath (b) NaN_3, water, room temperature, 4 h, 83–90% yield.

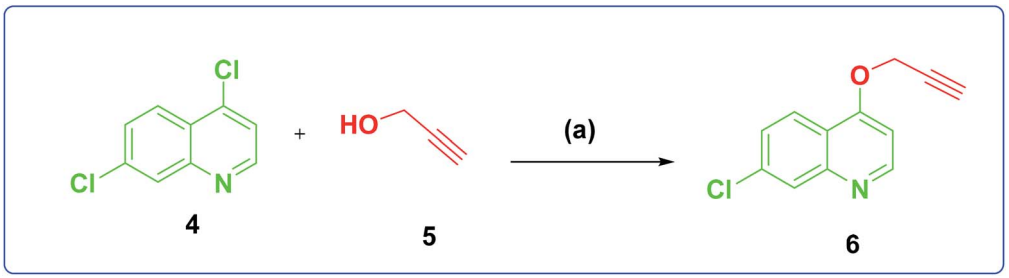

Scheme 2 Synthesis of 7-chloro-4-(prop-2-yn-1-yloxy)quinoline. Reagents and conditions: (a) NaH, dry DMF, propargyl, alcohol room temperature, 4 h, 70% yield.

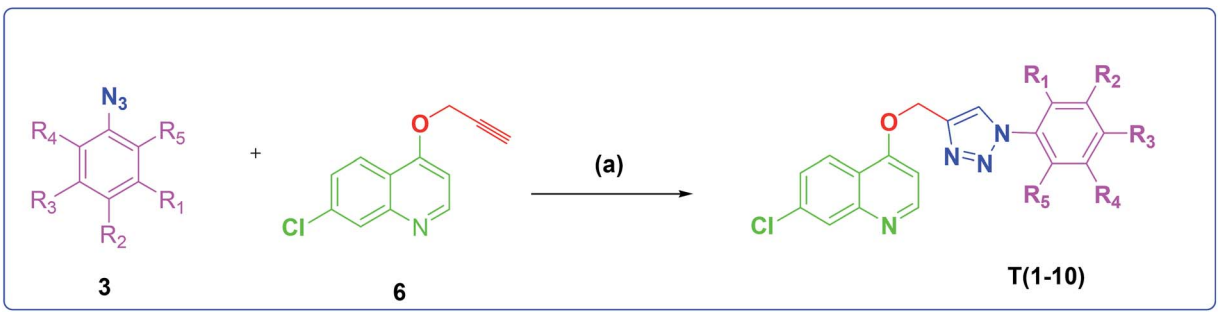

Scheme 3 Synthesis of different quinoline-triazole-based target compounds. Reagents and conditions: (a) $CuSO_4 \cdot 5H_2O$, sodium ascorbate, (THF–H_2O, 1 : 2), 80 °C, 8 h.

benzene. **T1** containing trifluoromethyl, showed inhibition of FP2 with (IC_{50} 26.59 μM). **T6** having fluoro group at position 3 of benzene ring and **T2** having chloro and fluoro groups, showed almost same inhibition for FP2 activity with IC_{50} values in the range of (45 μM). To distinguish the effect of different substituents on the benzene ring, compound **T10** was designed to have an unsubstituted benzene ring and its FP2 inhibition was found to be (58.46 μM). The compound **T5** containing *o*-fluoro benzene attached to the triazole core structure, exhibited exceptionally low inhibitory activity of the value of (107.32 μM) in comparison to other compounds of the series. Further, *in silico* studies of all the compounds were carried out with FP2 to bring more clarity in understanding their mode of action and more importantly, the *in vitro* results showed a good agreement with the *in silico* studies.

All the synthesized compounds were subsequently analyzed for their antimalarial activities in an *in vitro P. falciparum* 3D7 culture. As shown in Table 2, compound **T4** containing difluoro benzene ring attached to the triazole core moiety, inhibited *P. falciparum* with an EC_{50} value 21.89 μM. Furthermore, compound **T1** exhibited second best inhibition of *P. falciparum* 3D7 culture with EC_{50} 49.50 μM. Almost similar results EC_{50} 49.88 μM were found for **T7** containing nitro group at para position in the benzene ring. Compound **T10** with unsubstituted benzene ring inhibited the parasite growth in the range of 57.63 μM. Similar EC_{50} value ~57.86 were observed for **T6** compound containing *p*-fluoro benzene attached to the main trizole moiety. **T5** having *o*-fluoro benzene group, displayed the parasite development inhibition, EC_{50} 49.50 μM. **T9**, **T3** and **T2**

Table 2 *In vitro* inhibitory effect of quinoline-triazole based target compounds against recombinant FP2 and *P. falciparum* 3D7 (EC_{50}) growth *in vitro*

S. no.	Compound	Inhibition of FP2 IC_{50} (μM)	Std. error	Inhibition of *P. falciparum* EC_{50} (μM)	Std. error
1	**T1**	26.59	5.45	49.50	10.54
2	**T2**	45.08	9.46	405.64	398.80
3	**T3**	25.38	3.18	159.22	150.16
4	**T4**	25.64	4.13	**21.89**	**4.51**
5	**T5**	107.32	135.24	66.57	45.08
6	**T6**	45.78	18.98	57.86	183.93
7	**T7**	**16.16**	**3.03**	49.88	7.41
8	**T8**	25.37	1.94	51.71	8.57
9	**T9**	20.9	4.15	146.98	345.29
10	**T10**	58.46	19.07	57.63	14.02

disclosed lowest ability to inhibit the parasite development with EC_{50} values 146.98 μM, 159.22 μM and 405.64 μM, respectively.

2.3.2. Effect of quinoline-triazole based derivatives on parasite development. Cysteine protease inhibitors are well known to cause morphological and developmental abnormalities, mainly in the food vacuole of the parasites.[10] Since triazole-based target compounds affect FP2 activity, we next analyzed the effect of these compounds on the morphology of the 3D7 *Plasmodium* parasites. Briefly, the ring stage (8–10 h) parasites were treated with compounds **T7** or **T4** compounds or solvent alone as a control. In the control samples, the parasites grew normally from ring stage to trophozoite stage, and subsequently developed into the schizont stage and merozoites. These merozoites reinvaded fresh RBC to form rings. Cultures treated with a known cysteine protease inhibitor such as **E-64** (10 μM) showed severe food vacuole abnormalities at trophozoite stage and clumps of malarial pigment were observed, suggesting abrogation of hemozoin formation in these parasites. No new ring formation was observed in **E-64** treated parasites. *P. falciparum* cultures treated with compounds **T7** or **T4** at their IC_{50} value concentration also showed morphological and food-vacuole abnormalities followed by developmental arrest at the trophozoite stage, however the effect was less severe than **E-64** as we observed few new rings in **T7** or **T4** treated parasite (Fig. 5).

3. Conclusion

In the present study, a set of 10 triazole-quinoline derivatives (**T1–T10**) were computationally designed, synthesized and evaluated for FP2 inhibition and growth and development of *P. falciparum*. ParDOCK was used for docking and scoring purposes. The designed compounds were synthesized in the wet lab using click chemistry approach. Since the triazole scaffold is extremely versatile and has been featured in several clinically used drugs hence it once again evidenced to be a better drug candidate in the malaria treatment. In addition, quinoline moiety also verified to be a potential anti-malarial moiety. Generally, fluoro substituted triazole-quinoline molecules exhibited better enzyme inhibition as well as parasite growth and development inhibition. Computationally, compound **T7**, containing nitrobenzene attached to the triazole core structure exhibited the more negative binding free energy (-7.91 kcal mol^{-1}) with the target enzyme FP2 in the series, while as the standard inhibitor of FP2, **E64** exhibited binding energy of (-6.14 kcal mol^{-1}). The aromatic π electron cloud of triazole of **T7** was observed to interact with Trp43 *via* π–π stacking. The nitrogen of triazole formed a H-bond with Asn81 and oxygen of nitrobenzene of **T7** showed a H-bond with Cys39 with bond length of 2 Å. Compound **T7** displayed best inhibition of FP2 while as, **T4** containing difluoro benzene attached to the triazole ring arrested the development of *P. falciparum* at the trophozoite stage and showed morphological and food-vacuole abnormalities. The *in silico* and experimental results correlate

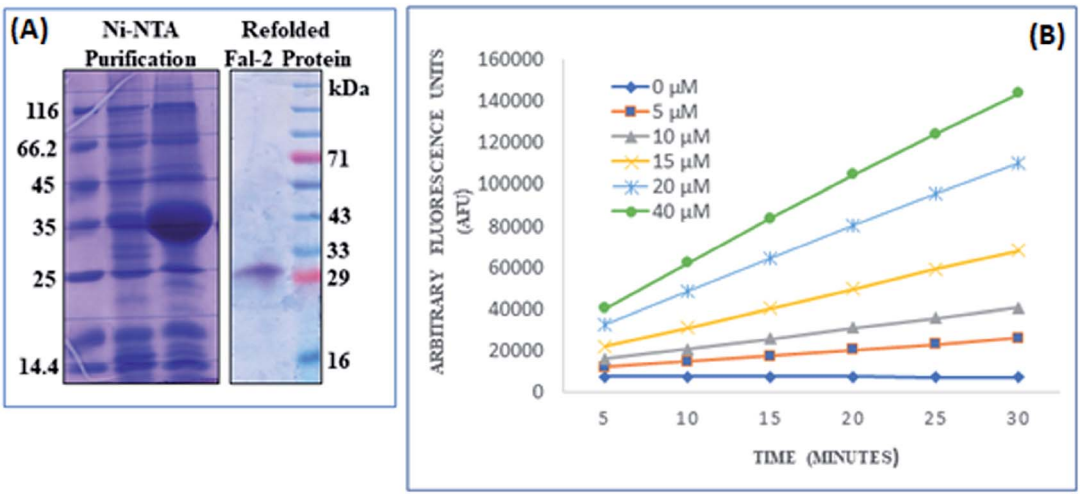

Fig. 4 Recombinant FP2 protein expression and activity analysis: (A) FP2 protein was expressed in *E. coli* cells and purification was done with Ni^{2+}-NTA column followed by refolding process. (B) Activity analysis of refolded FP2 using ZFR-AMC as substrate on dose dependent manner over a period of 30 min was measured at pH 5.5.

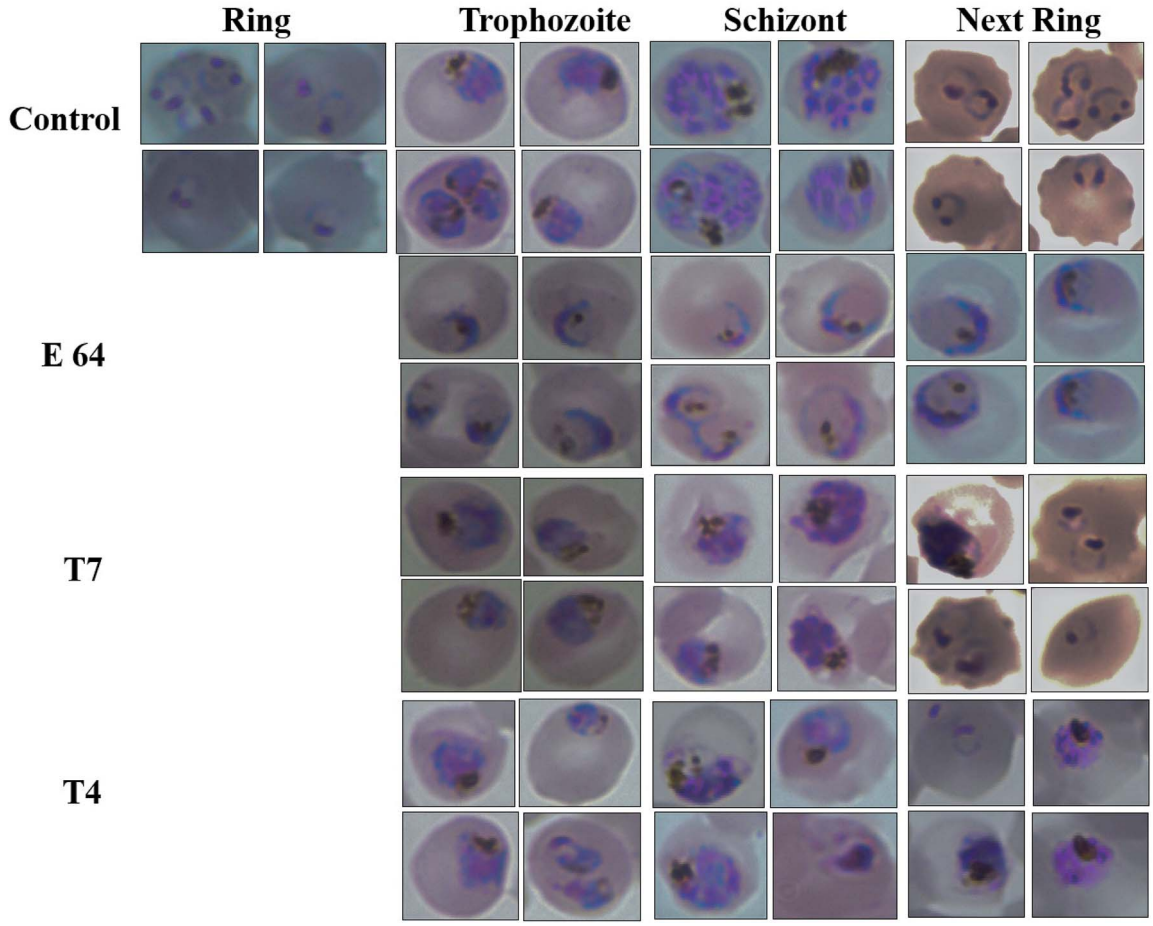

Fig. 5 Effect of E-64, compounds T7 and T4 on the growth and development of *P. falciparum*. Light microscopy images of parasitized red blood cells at different time points after the treatment with E64, T7 and T4.

to each other. These results make a clear clue for the usage of triazole and quinoline moieties in the development of future drugs to eradicate malaria completely.

4. Experimental section

4.1. Docking protocol

Protein Data Bank (http://www.rcsb.org)[64] was used as a source for obtaining the crystal structure of FP2 (PDB ID 3BPF) in pdb format which was further submitted along with the ligand molecules to ParDOCK module of Sanjeevini[65,66] for molecular docking and scoring determinations. It is important to mention that ParDOCK is an inclusive drug design suite which functions on physicochemical descriptors by integrating several protocols and deals protein and the ligands at the atomic level. The ligand was produced in its input pose for the calculation. Addition of hydrogen to the ligand was accomplished using xleap of AMBER[67] and geometry optimization and partial charge calculations were performed *via* AM1-BCC procedure. The docked structures are energy minimized using the sander module of AMBER and scored using scoring function Bappl[68] which is an all atom-based scoring function consisting electrostatics, van der Waals hydrophobicity, loss of conformational entropy of protein side chains after complexation. In addition to ParDOCK, AutoDock Vina program[60] (version 1.5.6) was used to validate the docking results and detailed information is provided in the ESI section.†

PyMOL, a molecular visualizing software was used to visualize the molecular interactions. Weak non-covalent interactions like π–π stacking interaction and H-bonding were observed between the active site residues of FP2 and the ligand molecules lying within a range of 2 Å. In addition, the binding free energy of the molecules was calculated based on which the molecules were screened.

4.2. Chemistry

The chemicals, reagents and solvents used during the synthesis and characterization of the compounds were brought from the commercial vendors like Sigma Aldrich, Alfa-Aesar and Spectrochem Pvt. Ltd. (India). ^{1}H NMR and ^{13}CNMR spectra were observed on Bruker 75 and 300 MHz spectrophotometer using deuterated solvents ($CDCl_3$, δ 7.26; DMSO-d6 δ 2.54) and multiplicities of NMR signals are designated as s (singlet), d (doublet), dd (double doublet), t (triplet), q (quartet), m (multiplet, for unresolved lines). Chemical shifts were showed in δ (ppm) and tetramethylsilane was used as the internal

standard. Mass spectra were recorded on UPLC XEVO G2-XS QTOF Spectrometer (HRMS) instrument. Thin layer chromatography was performed with Merck silica gel (60–120 and F254) aluminum-coated sheets of 0.25 mm thickness. Spots on these were observed in short (254 nm) with ultraviolet light and long (365 nm) wavelengths. Elemental analyses were obtained on Elementar Vario analyser. Elemental analyses of the compounds were found to be within ±0.4% of the theoretical values. The purity of tested compounds was >95%.

4.2.1. General procedure for the synthesis of compound 3a–3j. Different anilines (20 mmol) were added to a stirring solution of HCl (3 N, 20 mL) in an ice bath, $NaNO_2$ (30 mmol) dissolved in 30 mL water was added drop wise. The reaction mixture was stirred for 40 minutes. Sodium azide (40 mmol) dissolved in 50 mL water was added drop wise. Then, the system was stirred for 8 h at room temperature. The mixture was extracted with ethyl acetate and the organic phase was washed with dilute HCl thrice to remove the residual phenylalanine and the combined organic layer was dried over Na_2SO_4. The organic layer was concentrated by rotavapor. The crude product was triturated in EtOAc/hexane 1 : 1 v/v, isolated by filtration and air dried to obtain pure compounds **3a–3j**.

4.2.2. General procedure for the synthesis of compound 6. A solution of propargyl alcohol (1.5 g, 0.026 mmol) and DMF (50 mL) could stirrer in an ice bath for 20 minutes. Sodium hydride (1.5 g, 0.06 mmol) was added to the propargyl alcohol-DMF solution in small instalments. After 30 minutes, was added 4,7-dichloroquinoline (5 g, 0.025 mmol) to the reaction mixture. The reaction mixture was stirring at room temperature for 4 h. The success of the reaction was confirmed by TLC. The reaction mixture quenched by ice cold water and the organic layer was obtained with ethyl acetate (100 mL × 3). The organic layer was dried using Na_2SO_4. The crude product was purified using column chromatography with eluting solvents: ethyl acetate/hexane = 20 : 80. The pure compound obtained was white colored powder.

4.2.3. General procedure for the synthesis of compounds T1–T10. Substituted azide (20 mg, 0.23 mmol) and alkyne (0.28 mmol) was dissolved in a mixed solvent system (THF–H_2O, 1 : 2). A freshly prepared aqueous solution of sodium ascorbate (0.12 mmol, 0.2 mL) was added followed by freshly prepared aqueous solution of $CuSO_4 \cdot 5H_2O$ (0.04 mmol, 0.2 mL). The yellowish reaction mixture was stirred at 80 °C. After the completion of the reaction, the reaction mixture was directly dried under vacuum and the crude material was purified by column chromatography ethyl acetate–hexane = 50 : 50. Yield of the desired product was found to be in the range of 60 to 80%.

*4.2.3.1. 7-Chloro-4-({1-[3-(trifluoro methyl)phenyl]-1H-1,2,3-triazol-4yl}methoxy) quinoline (**T1**).* Brown solid ($R_f = 0.3$ in pure ethyl acetate) mp 161–163 °C, 70% yield isolated after column chromatography. ^{1}H NMR (300 MHz, $CDCl_3$) δ 8.79 (d, J = 5.4 Hz, 1H), 8.24 (s, 1H), 8.13 (d, J = 9.00 Hz, 1H), 8.06 (d, J = 1.9 Hz, 1H), 8.00 (d, J = 7.5 Hz, 1H), 7.72 (m, J = 2H), 7.44 (dd, J = 8.7, 2.1 Hz, 1H), 7.27 (s, 1H), 6.99 (d, J = 5.4 Hz, 1H), 5.55 (s, 2H). ^{13}C NMR (75 MHz, $CDCl_3$) δ 174.86, 161.24, 151.85, 148.63, 143.58, 137.04, 136.32, 133.09, 132.65, 132.30, 131.76, 130.67, 126.92, 123.61, 123.43, 121.60, 119.50, 117.49, 101.47, 62.18. HRMS m/z: calcd for $C_{19}H_{12}ClF_3N_4O$ $[M + H]^+$ 404.0652 found 405.0716 elemental anal.: calcd: C, 56.47; H, 2.98; Cl, 8.57; F, 14.17; N, 13.75; O, 3.86.

*4.2.3.2. 7-Chloro-4-{[1-(3-chloro-4-fluorophenyl)-1H-1,2,3-triazol-4-yl]methoxy} quinoline (**T2**).* Yellow solid ($R_f = 0.3$ in pure ethyl acetate) mp 185–187 °C, 60% yield obtained after column chromatography. ^{1}H NMR (400 MHz, $CDCl_3$) δ 8.76 (d, J = 5.6 Hz, 1H), 8.13 (s, 1H), 8.09 (d, J = 8.8 Hz, 1H), 8.03 (d, J = 2.0 Hz, 1H), 7.85 (dd, J = 9.2, 2.0 Hz, 1H), 7.64 (m, 1H), 7.41 (dd, J = 8.9, 2.0 Hz, 1H), 7.34–7.27 (m, 1H), 6.96 (d, J = 5.2 Hz, 1H), 5.50 (s, 2H). ^{13}C NMR (101 MHz, $CDCl_3$) δ 175.78, 161.30, 152.05, 148.86, 143.64, 136.50, 127.12, 127.08, 123.50, 123.28, 121.63, 120.55, 120.48, 119.64, 118.00, 117.77, 101.58, 62.27. HRMS m/z: calcd for $C_{18}H_{11}Cl_2FN_4O$ $[M + H]^+$ 388.0294 found 389.0302 elemental anal.: calcd: C, 55.37; H, 2.76; Cl, 18.13; F, 4.79; N, 14.31; O, 4.02.

*4.2.3.3. 7-Chloro-4-{[1-(2,4-difluorophenyl)-1H-1,2,3-triazol-4-yl]methoxy} quinoline (**T3**).* White chalk (R_f = 0.5 in pure ethyl acetate) mp 173–175 °C, 70% yield obtained after column chromatography. ^{1}H NMR (400 MHz, $CDCl_3$) δ 8.75 (d, J = 5.2 Hz, 1H), 8.19 (d, J = 2.4 Hz, 1H), 8.11 (d, J = 9.2 Hz, 1H), 8.01 (d, J = 1.6 Hz, 1H), 7.98–7.92 (m, 1H), 7.41 (dd, J = 9.2, 2.4 Hz, 1H), 7.10–7.04 (m, 2H), 6.96 (d, J = 5.2 Hz, 1H), 5.51 (s, 2H). ^{13}C NMR (101 MHz, $CDCl_3$) δ 160.91, 152.53, 149.78, 143.22, 136.04, 127.94, 126.85, 126.26, 124.54, 124.46, 123.50, 119.75, 113.03, 113.00, 112.81, 112.77, 101.54, 62.15 HRMS m/z:calcd $C_{18}H_{11}ClF_2N_4O$ $[M + H]^+$ 372.7559 found 373.0706 elemental anal.:-calcd: C, 58.00; H, 2.88; Cl, 9.33; F, 10.28; N, 15.12; O, 4.38.

*4.2.3.4. 7-Chloro-4-{[1-(3,4-difluorophenyl)-1H-1,2,3-triazol-4-yl]methoxy} quinoline (**T4**).* Brown solid (R_f = 0.5 in pure ethyl acetate) mp 177–179 °C, 80% yield obtained after column chromatography. ^{1}H NMR (300 MHz, CDCl3) δ 8.78 (d, J = 5.4 Hz, 1H), 8.15 (s, 1H), 8.11 (d, J = 5.1 Hz, 1H), 8.04 (s, 1H), 7.73–7.66 (m, 1H), 7.51 (d, J = 9.0 Hz, 1H), 7.44 (d, J = 8.7 Hz, 1H), 7.36 (d, J = 8.4 Hz, 1H), 6.97 (d, J = 5.4 Hz, 1H), 5.53 (s, 2H). ^{13}C NMR (75 MHz, $CDCl_3$) δ 160.70, 152.44, 149.76, 143.81, 135.81, 133.06, 127.93, 126.74, 123.32, 121.37, 119.63, 118.64, 118.40, 116.59, 110.95, 110.66, 101.45, 62.11. HRMS m/z: calcd $C_{18}H_{11}ClF_2N_4O$ $[M + H]^+$ 372.7559 found 373.0706. Elemental anal.: calcd: 47.11; H, 2.88; Cl, 9.42; F, 10.37; N, 15.21; O, 4.47.

*4.2.3.5. 7-Chloro-4-{[1-(2-fluorophenyl)-1H-1,2,3-triazol-4-yl] methoxy} quinoline (**T5**).* White (R_f = 0.5 in pure ethyl acetate) mp 180–182 °C, 80% yield isolated yield after flash column chromatography. ^{1}H NMR (300 MHz, $CDCl_3$) δ 8.80 (d, J = 5.1 Hz, 1H), 8.15 (d, J = 9.0 Hz, 1H), 8.09 (s, 1H), 8.06 (d, J = 1.8 Hz, 1H), 7.74 (dd, J = 9.0, 4.5 Hz, 2H), 7.45 (dd, J = 9.0, 1.8 Hz, 1H), 7.29–7.23 (m, 2H), 7.01 (d, J = 5.4 Hz, 1H), 5.54 (s, 2H). ^{13}C NMR (75 MHz, $CDCl_3$) δ 175.35, 161.23, 152.10, 149.03, 143.35, 136.34, 133.05, 127.22, 126.98, 123.43, 122.78, 122.66, 121.59, 119.66, 117.05, 116.74, 101.55, 62.30. HRMS m/z: calcd $C_{18}H_{12}ClFN_4O$ $[M + H]^+$ 354.0684 found 355.0793 HRMS m/z: calcd $C_{18}H_{12}ClFN_4O$ $[M + H]^+$ 354.0684 found 355.0682. Elemental anal.: calcd: C, 60.76; H, 3.23; Cl, 10.00; F, 5.25; N, 15.79; O, 4.14.

*4.2.3.6. 7-Chloro-4-{[1-(4-fluorophenyl)-1H-1,2,3-triazol-4-yl] methoxy} quinoline (**T6**).* White, (R_f = 0.4 in pure ethyl acetate) mp 155–157 °C, 66% yield obtained after column

chromatography. ^{1}H NMR (300 MHz, $CDCl_3$) δ 8.80 (d, J = 5.1 Hz, 1H), 8.15 (d, J = 9.0 Hz, 1H), 8.09 (s, 1H), 8.06 (d, J = 1.8 Hz, 1H), 7.74 (dd, J = 9.0, 4.5 Hz, 2H), 7.45 (dd, J = 9.0, 1.8 Hz, 1H), 7.29–7.23 (m, 2H), 7.01 (d, J = 5.4 Hz, 1H), 5.54 (s, 2H). ^{13}C NMR (75 MHz, $CDCl_3$) δ 175.35, 161.23, 152.10, 149.03, 143.35, 136.34, 133.05, 127.22, 126.98, 123.43, 122.78, 122.66, 121.59, 119.66, 117.05, 116.74, 101.55, 62.30. HRMS *m*/*z*: calcd $C_{18}H_{12}ClFN_4O$ $[M + H]^+$ 354.0684 found 355.0793 elemental anal.: calcd: C, 60.85; H, 3.32; Cl, 9.99; F, 5.63; N, 15.97; O, 4.42.

*4.2.3.7. 7-Chloro-4-{[1-(4-nitrophenyl)-1H-1,2,3-triazol-4-yl] methoxy} quinoline (**T7**).* Light yellow solid, (R_f = 0.3 in pure ethyl acetate) mp 166–168 °C, 72% yield obtained after column chromatography. ^{1}H NMR (300 MHz, $CDCl_3$) δ 8.79 (d, J = 5.1 Hz, 1H), 8.53 (s, 1H), 8.44 (d, J = 8.7 Hz, 1H), 8.18 (d, J = 8.7 Hz, 1H), 8.10 (d, J = 9.0 Hz, 2H), 8.02 (s, 1H), 7.46 (d, J = 9.0 Hz, 1H), 7.38 (s, 1H), 7.03 (d, J = 5.1 Hz, 1H), 5.56 (s, 2H). ^{13}C NMR (75 MHz, $CDCl_3$) δ 165.53, 157.39, 148.65, 145.87, 140.32, 132.44, 131.29, 130.23, 128.52, 127.44, 125.49, 106.60, 66.82, 45.41, 44.85, 44.30. HRMS *m*/*z*: calcd $C_{18}H_{12}ClN_5O_3$ $[M + H]^+$ 381.0629 found 382.0733 elemental anal.: calcd: C, 57.00; H, 3.35; Cl, 9.36; N, 18.43; O, 13.01.

*4.2.3.8. 7-Chloro-4-{[1-(4-methoxyphenyl)-1H-1,2,3-triazol-4-yl]methoxy} quinoline (**T8**).* Yellow solid powder, (R_f = 0.5 in pure ethyl acetate) mp 179–181 °C, 76% yield obtained after column chromatography. ^{1}H NMR (300 MHz, $CDCl_3$) δ 8.80 (d, J = 5.4 Hz, 1H), 8.15 (d, J = 9.0 Hz, 1H), 8.06 (s, 2H), 7.65 (d, J = 9.0 Hz, 2H), 7.45 (d, J = 9.0 Hz, 1H), 7.27 (s, 1H), 7.04 (d, J = 8.7 Hz, 2H), 5.53 (s, 2H), 3.88 (s, 3H). ^{13}C NMR (75 MHz, $CDCl_3$) δ 175.36, 161.39, 160.10, 151.97, 148.75, 142.87, 136.33, 130.13, 126.93, 123.52, 122.29, 121.68, 119.65, 114.86, 101.57, 62.37, 55.64. HRMS *m*/*z*: calcd $C_{19}H_{15}ClN_4O_2$ $[M + H]^+$ 366.0884 found 367.0927 elemental anal.: calcd: C, 62.03; H, 4.02; Cl, 10.00; N, 15.55; O, 8.54.

*4.2.3.9. 7-Chloro-4-{[1-(2-methylphenyl)-1H-1,2,3-triazol-4-yl] methoxy} quinoline (**T9**).* Snow white solid, (R_f = 0.5 in pure ethyl acetate) mp 180–182 °C, 73% yield obtained after column chromatography. ^{1}H NMR (300 MHz, $CDCl_3$) δ 8.80 (d, J = 5.1 Hz, 1H), 8.12 (dd, J = 16.5, 9.0 Hz, 3H), 7.62 (d, J = 8.1 Hz, 2H), 7.45 (d, J = 8.4 Hz, 1H), 7.33 (d, J = 7.9 Hz, 2H), 7.01 (d, J = 4.8 Hz, 1H), 5.53 (s, 2H), 2.43 (s, 3H). ^{13}C NMR (75 MHz, $CDCl_3$) δ 175.33, 161.35, 152.04, 148.90, 142.98, 139.39, 136.30, 134.47, 130.34, 127.06, 126.94, 123.50, 121.47, 120.56, 119.75, 119.67, 101.56, 62.38, 21.05. HRMS *m*/*z*: calcd $C_{19}H_{15}ClN_4O$ $[M + H]^+$ 350.0934 found 351.0924 elemental anal.: calcd: C, 65.05; H, 4.30; Cl, 10.11; N, 16.00; O, 5.01.

*4.2.3.10. 7-Chloro-4-[(1-phenyl-1H-1,2,3-triazol-4-yl)methoxy] quinoline (**T10**).* White, (R_f = 0.3 in pure ethyl acetate) mp 168–170 °C, 71% yield obtained after column chromatography. ^{1}H NMR (300 MHz, $CDCl_3$) δ 8.77 (d, J = 5.1 Hz, 1H), 8.15 (d, J = 5.7 Hz, 1H), 8.03 (s, 1H), 7.76 (d, J = 7.8 Hz, 2H), 7.57–7.43 (m, 4H), 7.27 (s, 1H), 6.99 (d, J = 5.4 Hz, 1H), 5.53 (s, 2H). ^{13}C NMR (75 MHz, $CDCl_3$) δ 160.87, 152.44, 149.69, 143.31, 136.78, 135.91, 129.86, 129.15, 127.82, 126.70, 123.43, 121.44, 120.64, 119.70, 101.51, 62.27. HRMS *m*/*z*: calcd $C_{18}H_{13}ClN_4O$ $[M + H]^+$ 336.0778 found 337.0790 elemental anal.: calcd: C, 64.00; H, 4.00; Cl, 10.35; N, 17.00; O, 4.90.

4.3. Procedures for biological assays

4.3.1. Recombinant FP2 protein preparation. Recombinant FP2 was prepared according to the method described by Shenai, *et al.*[62] and Kumar, *et al.*[63] with slight modification. Briefly, bacteria containing the PRSET-A FP2 plasmid were grown to mid-log phase and induced with isopropyl-1-thio-β-D-galactopyranoside (IPTG, 1 mM) for 5 h at 37 °C. IPTG induced pellet were suspended in ice-cold native buffer (50 mM NaH_2PO_4 and 100 mM NaCl). Added lysozyme (10 μL/1 mL; 1 mg mL^{-1} (FC); stock 100 mg mL^{-1}), mixed well and keep in ice for 30 min. Sonicated and centrifuged at 15 000 rpm for 45 min at 4 °C. The pellet was washed twice with native buffer. Finally, the pellet was solubilized in UB [8 M urea, 20 mM Tris, 250 mM NaCl, pH 8.0]; (5 mL g^{-1} of inclusion body pellet) at room temperature for 60 min with gentle stirring. The insoluble material was separated by centrifuging at 15 000 rpm for 60 min at 4 °C. Added imidazole to 10 mM, Triton X-100 to 1% supernatant. In order to purify of recombinant protein, supernatant was incubated overnight at a temperature of 4 °C with a nickel-nitrilotriacetic acid (Ni-NTA) resin. The resin was loaded on the column and it was washed with 10 bed volumes each of UB. Finally, the bound protein was eluted in UB with 250 mM imidazole and measured by the bicinchoninic acid assay. For refolding, the fractions containing FP2 protein were pooled in ice-cold refolding buffer and diluted 100-fold using Tris–HCl (100 mM), 1 mM EDTA, 20% glycerol, 250 mM L-arginine, 1 mM GSH, 1 mM GSSG, pH 8.0. The mixture was incubated with moderate stirring at 4 °C for 24 h, and concentrated to 25 mL using a stirred cell with a 10 kDa cut-off membrane (Pellicon XL device, Millipore) at 4 °C. The sample was then filtered using a 0.22 mm syringe filter. The purified and concentrated protein was quantified using bicinchoninic acid assay.

4.3.2. Enzyme assay and kinetic analysis. FP2 activity was carried out as described previously by Kumar, *et al.*[63] Briefly, in 96 well plate 200 μL of assay buffer (100 mM sodium acetate pH 5.5, 10 mM DTT) containing 15 μM FP2 enzyme, 10 μM fluorogenic substrate benzyloxycarbonyl-Phe-Arg-7-amino-4-methylcoumarin hydrochloride (ZFR-AMC) was added and the release of 7-amino-4-methyl coumarin (AMC) was monitored (excitation 355 nm; emission 460 nm) over 30 min at RT using a LS50B PerkinElmer fluorimeter. To analyze the effect of inhibitors on enzyme activity, recombinant FP2 was pre-incubated with different concentration of each inhibitor for 10 min at room temperature. Remaining activity was determined using the fluorogenic substrate. Kinetic constants k_m, V_{max}, and IC_{50} values were determined using PRISM software (Graph Pad, San Diego).

4.3.3. *P. falciparum* culture and inhibition assay. *P. falciparum* strain 3D7 was cultured with human erythrocytes (4% hematocrit) in RPMI media (Invitrogen) supplemented with 0.5% albumax and 4% hematocrit using a protocol described previously.[69] Cultures were synchronized by repeated sorbitol treatment following Lambros and Vanderberg.[70] Each growth inhibition assay was performed in triplicate, and the experiment was repeated twice. Each well contained 0.2 mL of complete media (RPMI (Invitrogen) with 0.5% albumax), 2%

hematocrit, and the parasitemia adjusted to ≤1%. The compound was added to the synchronized 8–10 h ring parasite cultures at the desired final concentration (0–100 μM), and same amount of solvent (DMSO) was added to the control wells. The cultures were allowed to grow for 52 h. Parasite growth was assessed by DNA fluorescent dye-binding assay using SYBR green (Sigma) following Smilkstein, *et al.*[71]

Conflicts of interest

There are no conflicts to declare.

Acknowledgements

A. S. would like to acknowledge University Grants Commission, Government of India for RGNF Senior Research Fellowship.

References

1 J. N. Burrows, E. Burlot, B. Campo, S. Cherbuin, S. Jeanneret, D. Leroy, T. Spangenberg, D. Waterson, T. N. Wells and P. Willis, *Parasitology*, 2014, **141**, 128–139.
2 E. L. Flannery, A. K. Chatterjee and E. A. Winzeler, *Nat. Rev. Microbiol.*, 2013, **11**, 849–862.
3 A. R. Renslo, *ACS Med. Chem. Lett.*, 2013, **4**, 1126–1128.
4 M. A. Phillips, J. N. Burrows, C. Manyando, R. H. van Huijsduijnen, W. C. Van Voorhis and T. N. C. Wells, *Nat. Rev. Dis. Primers*, 2017, **3**, 17050.
5 D. E. Goldberg, A. F. Slater, A. Cerami and G. B. Henderson, *Proc. Natl. Acad. Sci. U. S. A.*, 1990, **87**, 2931–2935.
6 E. Deu, *FEBS J.*, 2017, **284**, 2604–2628.
7 *Cysteine Proteases of Pathogenic Organisms*, ed. M. W. Robinson and J. P. Dalton, Springer US, Boston, MA, 2011, vol. 712.
8 M. Marco and J. M. Coterón, *Curr. Top. Med. Chem.*, 2012, **12**, 408–444.
9 S. C. Stolze, E. Deu, F. Kaschani, N. Li, B. I. Florea, K. H. Richau, T. Colby, R. A. L. van der Hoorn, H. S. Overkleeft, M. Bogyo and M. Kaiser, *Chem. Biol.*, 2012, **19**, 1546–1555.
10 P. S. Sijwali and P. J. Rosenthal, *Proc. Natl. Acad. Sci. U. S. A.*, 2004, **101**, 4384–4389.
11 A. Stoye, A. Juillard, A. H. Tang, J. Legac, J. Gut, K. White, S. A. Charman, P. J. Rosenthal, G. E. R. Grau, N. H. Hunt and R. J. Payne, *J. Med. Chem.*, 2019, **62**, 5562–5578.
12 T. B. de Carvalho, T. C. G. Oliveira-Sequeira and S. Guimaraes, *Rev. Inst. Med. Trop. Sao Paulo*, 2014, **56**, 43–47.
13 E. Sonoiki, C. L. Ng, M. C. S. Lee, D. Guo, Y.-K. Zhang, Y. Zhou, M. R. K. Alley, V. Ahyong, L. M. Sanz, M. J. Lafuente-Monasterio, C. Dong, P. G. Schupp, J. Gut, J. Legac, R. A. Cooper, F.-J. Gamo, J. DeRisi, Y. R. Freund, D. A. Fidock and P. J. Rosenthal, *Nat. Commun.*, 2017, **8**, 14574.
14 R. Ettari, N. Micale, T. Schirmeister, C. Gelhaus, M. Leippe, E. Nizi, M. E. Di Francesco, S. Grasso and M. Zappalà, *J. Med. Chem.*, 2009, **52**, 2157–2160.
15 J. M. Coterón, D. Catterick, J. Castro, M. J. Chaparro, B. Díaz, E. Fernández, S. Ferrer, F. J. Gamo, M. Gordo, J. Gut, L. de las Heras, J. Legac, M. Marco, J. Miguel, V. Muñoz, E. Porras, J. C. de la Rosa, J. R. Ruiz, E. Sandoval, P. Ventosa, P. J. Rosenthal and J. M. Fiandor, *J. Med. Chem.*, 2010, **53**, 6129–6152.
16 K. N. P. G. Allangba, M. Keita, R. Kre N'Guessan, E. Megnassan, V. Frecer and S. Miertus, *J. Enzyme Inhib. Med. Chem.*, 2019, **34**, 547–561.
17 N. Sharma, D. Mohanakrishnan, A. Shard, A. Sharma, Saima, A. K. Sinha and D. Sahal, *J. Med. Chem.*, 2012, **55**, 297–311.
18 I. Ravish and N. Raghav, *RSC Adv.*, 2015, **5**, 50440–50453.
19 H. Wei, J. Ruan and X. Zhang, *RSC Adv.*, 2016, **6**, 10846–10860.
20 J. E. Olson, G. K. Lee, A. Semenov and P. J. Rosenthal, *Bioorg. Med. Chem.*, 1999, **7**, 633–638.
21 P. J. Rosenthal, G. K. Lee and R. E. Smith, *J. Clin. Invest.*, 1993, **91**, 1052–1056.
22 R. Ettari, F. Bova, M. Zappalà, S. Grasso and N. Micale, *Med. Res. Rev.*, 2010, **30**, 136–167.
23 G. C. Tron, T. Pirali, R. A. Billington, P. L. Canonico, G. Sorba and A. A. Genazzani, *Med. Res. Rev.*, 2008, **28**, 278–308.
24 S. G. Agalave, S. R. Maujan and V. S. Pore, *Chem.–Asian J.*, 2011, **6**, 2696–2718.
25 A. D. Moorhouse, A. M. Santos, M. Gunaratnam, M. Moore, S. Neidle and J. E. Moses, *J. Am. Chem. Soc.*, 2006, **128**, 15972–15973.
26 X.-L. Wang, K. Wan and C.-H. Zhou, *Eur. J. Med. Chem.*, 2010, **45**, 4631–4639.
27 R. P. Tripathi, A. K. Yadav, A. Ajay, S. S. Bisht, V. Chaturvedi and S. K. Sinha, *Eur. J. Med. Chem.*, 2010, **45**, 142–148.
28 X. Li, Y. Lin, Q. Wang, Y. Yuan, H. Zhang and X. Qian, *Eur. J. Med. Chem.*, 2011, **46**, 1274–1279.
29 A. Montagu, V. Roy, J. Balzarini, R. Snoeck, G. Andrei and L. A. Agrofoglio, *Eur. J. Med. Chem.*, 2011, **46**, 778–786.
30 B. Fang, C.-H. Zhou and X.-C. Rao, *Eur. J. Med. Chem.*, 2010, **45**, 4388–4398.
31 N. Devender, S. Gunjan, R. Tripathi and R. P. Tripathi, *Eur. J. Med. Chem.*, 2017, **131**, 171–184.
32 F. Shah, P. Mukherjee, J. Gut, J. Legac, P. J. Rosenthal, B. L. Tekwani and M. A. Avery, *J. Chem. Inf. Model.*, 2011, **51**, 852–864.
33 C. Teixeira, J. R. B. Gomes and P. Gomes, *Curr. Med. Chem.*, 2011, **18**, 1555–1572.
34 F. Shah, Y. Wu, J. Gut, Y. Pedduri, J. Legac, P. J. Rosenthal and M. A. Avery, *MedChemComm*, 2011, **2**, 1201.
35 Y.-Q. Hu, S. Zhang, F. Zhao, C. Gao, L.-S. Feng, Z.-S. Lv, Z. Xu and X. Wu, *Eur. J. Med. Chem.*, 2017, **133**, 255–267.
36 L.-S. Feng, M.-L. Liu, S. Zhang, Y. Chai, B. Wang, Y.-B. Zhang, K. Lv, Y. Guan, H.-Y. Guo and C.-L. Xiao, *Eur. J. Med. Chem.*, 2011, **46**, 341–348.
37 S. Zhang, Z. Xu, C. Gao, Q.-C. Ren, L. Chang, Z.-S. Lv and L.-S. Feng, *Eur. J. Med. Chem.*, 2017, **138**, 501–513.
38 Z. Xu, S. Zhang, C. Gao, J. Fan, F. Zhao, Z.-S. Lv and L.-S. Feng, *Chin. Chem. Lett.*, 2017, **28**, 159–167.
39 X.-D. Jia, S. Wang, M.-H. Wang, M.-L. Liu, G.-M. Xia, X.-J. Liu, Y. Chai and H.-W. He, *Chin. Chem. Lett.*, 2017, **28**, 235–239.

40 S. K. Puri and G. P. Dutta, *Trans. R. Soc. Trop. Med. Hyg.*, 1990, **84**, 759–760.
41 A. P. Gorka, J. N. Alumasa, K. S. Sherlach, L. M. Jacobs, K. B. Nickley, J. P. Brower, A. C. de Dios and P. D. Roepe, *Antimicrob. Agents Chemother.*, 2013, **57**, 356–364.
42 D. C. Warhurst, J. C. Craig, I. S. Adagu, R. K. Guy, P. B. Madrid and Q. L. Fivelman, *Biochem. Pharmacol.*, 2007, **73**, 1910–1926.
43 A. C. Chou, R. Chevli and C. D. Fitch, *Biochemistry*, 1980, **19**, 1543–1549.
44 A. F. G. Slater and A. Cerami, *Nature*, 1992, **355**, 167–169.
45 T. J. Egan, D. C. Ross and P. A. Adams, *FEBS Lett.*, 1994, **352**, 54–57.
46 D. J. Sullivan, I. Y. Gluzman, D. G. Russell and D. E. Goldberg, *Proc. Natl. Acad. Sci. U. S. A.*, 1996, **93**, 11865–11870.
47 L. B. Casabianca, J. B. Kallgren, J. K. Natarajan, J. N. Alumasa, P. D. Roepe, C. Wolf and A. C. de Dios, *J. Inorg. Biochem.*, 2009, **103**, 745–748.
48 L. B. Casabianca, D. An, J. K. Natarajan, J. N. Alumasa, P. D. Roepe, C. Wolf and A. C. de Dios, *Inorg. Chem.*, 2008, **47**, 6077–6081.
49 A. Dorn, S. R. Vippagunta, H. Matile, C. Jaquet, J. L. Vennerstrom and R. G. Ridley, *Biochem. Pharmacol.*, 1998, **55**, 727–736.
50 S. Verma, S. Pandey, P. Agarwal, P. Verma, S. Deshpande, J. K. Saxena, K. Srivastava, P. M. S. Chauhan and Y. S. Prabhakar, *RSC Adv.*, 2016, **6**, 25584–25593.
51 A. Mahindra, R. P. Gangwal, S. Bansal, N. E. Goldfarb, B. M. Dunn, A. T. Sangamwar and R. Jain, *RSC Adv.*, 2015, **5**, 22674–22684.
52 B. C. Pérez, C. Teixeira, M. Figueiras, J. Gut, P. J. Rosenthal, J. R. B. Gomes and P. Gomes, *Eur. J. Med. Chem.*, 2012, **54**, 887–899.
53 M. C. Lombard, D. D. N'Da, J. C. Breytenbach, N. I. Kolesnikova, C. Tran Van Ba, S. Wein, J. Norman, P. Denti, H. Vial and L. Wiesner, *Eur. J. Pharm. Sci.*, 2012, **47**, 834–841.
54 R. Kharb, P. C. Sharma and M. S. Yar, *J. Enzyme Inhib. Med. Chem.*, 2011, **26**, 1–21.
55 D. K. Yadav, R. Rai, N. Kumar, S. Singh, S. Misra, P. Sharma, P. Shaw, H. Pérez-Sánchez, R. L. Mancera, E. H. Choi, M. Kim and R. Pratap, *Sci. Rep.*, 2016, **6**, 38128.
56 D. E. V. Pires, T. L. Blundell and D. B. Ascher, *J. Med. Chem.*, 2015, **58**, 4066–4072.
57 H. Miyakoshi, S. Miyahara, T. Yokogawa, K. Endoh, T. Muto, W. Yano, T. Wakasa, H. Ueno, K. T. Chong, J. Taguchi, M. Nomura, Y. Takao, A. Fujioka, A. Hashimoto, K. Itou, K. Yamamura, S. Shuto, H. Nagasawa and M. Fukuoka, *J. Med. Chem.*, 2012, **55**, 6427–6437.
58 P. Filippakopoulos, J. Qi, S. Picaud, Y. Shen, W. B. Smith, O. Fedorov, E. M. Morse, T. Keates, T. T. Hickman, I. Felletar, M. Philpott, S. Munro, M. R. McKeown, Y. Wang, A. L. Christie, N. West, M. J. Cameron, B. Schwartz, T. D. Heightman, N. La Thangue, C. A. French, O. Wiest, A. L. Kung, S. Knapp and J. E. Bradner, *Nature*, 2010, **468**, 1067–1073.
59 A. Gupta, A. Gandhimathi, P. Sharma and B. Jayaram, *Protein Pept. Lett.*, 2007, **14**, 632–646.
60 O. Trott and A. J. Olson, *J. Comput. Chem.*, 2010, **31**, 455–461.
61 S. Kumar, A. Saini, J. Gut, P. J. Rosenthal, R. Raj and V. Kumar, *Eur. J. Med. Chem.*, 2017, **138**, 993–1001.
62 B. R. Shenai, P. S. Sijwali, A. Singh and P. J. Rosenthal, *J. Biol. Chem.*, 2000, **275**, 29000–29010.
63 A. Kumar, P. V. N. Dasaradhi, V. S. Chauhan and P. Malhotra, *Biochem. Biophys. Res. Commun.*, 2004, **317**, 38–45.
64 V. M. S. Gil and N. C. Oliveira, *J. Chem. Educ.*, 1990, **67**, 473.
65 B. Jayaram, T. Singh, G. Mukherjee, A. Mathur, S. Shekhar and V. Shekhar, *BMC Bioinf.*, 2012, **13**, S7.
66 T. Singh, D. Biswas and B. Jayaram, *J. Chem. Inf. Model.*, 2011, **51**, 2515–2527.
67 D. A. Pearlman, D. A. Case, J. W. Caldwell, W. S. Ross, T. E. Cheatham, S. DeBolt, D. Ferguson, G. Seibel and P. Kollman, *Comput. Phys. Commun.*, 1995, **91**, 1–41.
68 T. Jain and B. Jayaram, *FEBS Lett.*, 2005, **579**, 6659–6666.
69 W. Trager and J. B. Jensen, *Science*, 1976, **193**, 673–675.
70 C. Lambros and J. P. Vanderberg, *J. Parasitol.*, 1979, **65**, 418–420.
71 M. Smilkstein, N. Sriwilaijaroen, J. X. Kelly, P. Wilairat and M. Riscoe, *Antimicrob. Agents Chemother.*, 2004, **48**, 1803–1806.